Catalysis Today 180 (2012) 81–87

Contents lists available at ScienceDirect

Catalysis Today

journal homepage: www.elsevier.com/locate/cattod

Redox and catalytic properties of CuO/CeO_2 under $CO + O_2 + NO$: Promoting effect of NO on CO oxidation

A. Martínez-Arias[a,*], A.B. Hungría[b], A. Iglesias-Juez[a], M. Fernández-García[a], J.A. Anderson[c], J.C. Conesa[a], G. Munuera[d], J. Soria[a]

[a] Instituto de Catálisis y Petroleoquímica, CSIC, C/Marie Curie 2, Campus de Cantoblanco, 28049 Madrid, Spain
[b] Departamento de Ciencia de Materiales, Ingeniería, Metalúrgica y Química Inorgánica, Facultad de Ciencias, Universidad de Cádiz, 11510 Puerto Real, Cádiz, Spain
[c] Surface Chemistry and Catalysis Group, Department of Chemistry, University of Aberdeen, AB24 3UE Scotland, UK
[d] Universidad de Sevilla, C/Profesor García González s/n, Departamento de Química Inorgánica, 41012 Sevilla, Spain

ARTICLE INFO

Article history:
Received 21 December 2010
Received in revised form 1 February 2011
Accepted 4 February 2011
Available online 9 March 2011

Keywords:
Copper oxide
Ceria-based catalysts
CO oxidation
Nitric oxide reduction
Cu^{2+} and O_2^- EPR
Operando-DRIFTS

ABSTRACT

A CuO/CeO_2 catalyst has been studied with respect to its catalytic activity for CO oxidation under stoichiometric conditions employing either O_2 or O_2–NO mixture as oxidants. The obtained results are rationalised on the basis of analysis of redox properties upon interaction with CO and O_2–NO by EPR as well as by redox/catalytic analysis by *operando*-DRIFTS. These provide useful insight into the processes involved during NO reduction, for which two well differentiated steps associated to a change in the type of active centres during the course of the reaction are evidenced. Nevertheless, the most interesting result is related to observation of a novel promoting effect of NO on CO oxidation. This is explained mainly on the basis of DRIFTS results and appears to be associated with phenomena of adsorption/desorption of NO_x species at interfacial positions which apparently activate such interfacial region allowing formation of greater amounts of active reduced copper centres in the presence of NO.

1. Introduction

Catalysts based on ceria present a wide range of applications such as three-way catalysts for automobile exhaust gas emission control, removal of SO_x–NO_x from fluid catalytic cracking flue gases, electrocatalysts over fuel cell electrodes, and catalysts for various oxidation and hydrogenation reactions [1,2]. For most of these applications, ceria or related compounds (isostructural cerium-containing mixed oxides) are thought to operate mainly as redox state or structural promoters of the active metal (or metal oxides) with which they are in contact and/or as bifunctional promoter [1,3]. A noteworthy aspect of ceria-related oxides is that they can promote the activity of catalysts with in principle different functionalities such as precious metals (for instance, Rh, Pt, and Pd, typically present in TWC) and base metals or metal oxides [1,4–6].

Among the latter, outstanding activities, comparable to those exhibited by precious metal catalysts, are shown by copper (or copper oxide) catalysts in reactions of high technological interest like CO oxidation, preferential CO oxidation in H_2-rich streams (CO-PROX), methanol steam reforming, methanol synthesis from CO and H_2, or water–gas shift [4–12]. For processes involving CO oxidation, different hypotheses have been made to account for the synergetic effects observed upon establishment of interactions between highly dispersed copper oxide species and ceria-related oxides [4,6,13,14]. The existence of a correlation between the reducibility of the dispersed copper oxide species and the catalytic activity is well recognized [6,15,16]. In turn, it has been shown that the copper oxide active sites exhibit a facile redox interplay with both reducing and oxidizing reactants [6,15,17], compatible with proposals that the reaction follows a redox (Mars-van Krevelen type) mechanism [18,19], in contrast with earlier reports suggesting a stabilizing effect of ceria on certain redox states of copper as mainly responsible for the catalytic enhancement [4]. Additionally, it appears that such redox activity in the copper oxide component can involve concomitant redox changes in the ceria support [6,17,20,21], strongly suggesting that it is the CuO–CeO_2 interfacial region as a whole which is in fact involved on the CO oxidation catalytic activity [15,22–24], in reasonable agreement with earlier postulations [4,25,26].

Concerning NO reduction by CO on catalysts of this type, a recent study proposes there are two NO dissociation sites in Cu/CeO_2 catalyst mainly on the basis of NO-TPD results: oxygen vacancies in ceria, as indicated earlier [27], and metallic copper [28]. It is also proposed in that study that NO adsorbed on the former can be more easily dissociated to N_2 and N_2O than NO adsorbed on the latter [28]. On the other hand, Zhang et al. propose, mainly on the basis

* Corresponding author.
E-mail address: amartinez@icp.csic.es (A. Martínez-Arias).

0920-5861/$ – see front matter © 2011 Elsevier B.V. All rights reserved.
doi:10.1016/j.cattod.2011.02.014

of *in situ* DRIFTS analysis, two different mechanisms of NO reduction by CO over $Cu/Ce_xZr_{1-x}O_2$ catalysts, differing in the reaction temperature at which they operate, in correlation with observation of two well separated NO conversion steps during light-off ramp [29]. They propose in any case that active sites are related to Cu^+ species onto which NO molecules become activated, with ceria being involved in the mechanism through redox changes basically related to oxygen uptake/release processes [29]. Thus, for the low temperature process (323–523 K) they propose that N_2O or N_2 is essentially produced from coupling of two close nitrosyl species resulting from NO chemisorption at Cu^+ sites [29]. In contrast, the high temperature process is proposed to involve interaction of a Cu^+ nitrosyl with CO giving rise to Cu^+-chemisorbed isocyanate species, whose further interaction with either Cu^+ nitrosyls or monoatomic oxygen species coordinated to cerium cations gives rise to nitrogen [29].

Within this context, the present work intends to provide further insight into processes involved in the catalytic CO oxidation and NO reduction over a CuO/CeO_2 catalyst. For this purpose, catalytic activity tests and *in situ* DRIFTS spectroscopy under $CO + O_2$ and $CO + O_2 + NO$ are examined and compared in order to achieve further insight into the redox processes involved in CO oxidation as well as simultaneously analysing catalytic properties of the system for NO reduction in the presence of O_2. The results are complemented by redox analyses using EPR. Discussion is performed also on the basis of characterization of the system and redox properties provided by previous works [6,30–32]. Further evidence of the involvement of interfacial sites on the catalytic processes as well as mechanistic details of the processes involved in CO oxidation and NO reduction over this type of catalysts will be revealed. In particular, a change in the rate of NO reduction is revealed and directly related, on the basis of *operando* DRIFTS, to a change in the type of active site during the course of the reaction. In addition, most interestingly, a novel promoting effect of NO acting as gaseous promoter for CO oxidation is revealed and explained on the basis of mainly *operando*-DRIFTS experiments.

2. Experimental

2.1. Materials

The CeO_2 support was prepared by a microemulsion method by mixing two reverse microemulsions containing aqueous phases prepared by dissolving cerium (III) nitrate hexahydrate for the first and tetramethylammonium hydroxyde pentahydrate for the second, dispersed in an organic solvent (*n*-heptane), using Triton X-100 (Aldrich) as surfactant and hexanol as co-surfactant. Following centrifugation, decanting and rinsing of the resulting solid with methanol, it was dried at 383 K for 24 h and finally calcined in air at 773 K for 2 h. Further details on the preparation and characteristics of this support can be found elsewhere [21,30]. The catalyst of copper supported on CeO_2 (hereafter referred to as CuC) was prepared by incipient wetness impregnation of the CeO_2 support using an aqueous solution of $Cu(NO_3)_2{\cdot}3H_2O$ (to give a final copper loading of 1 wt.%, representing *ca.* 157 μmol of Cu per gram of catalyst). The resulting material was dried overnight at 383 K and subsequently calcined in air at 773 K for 2 h.

All the gases employed were of commercial purity (CO: 99.9%; O_2: 99.99%; NO: 98.5%, with 1% NO_2 and 0.5% N_2O as the main impurities) and, for EPR experiments, were further purified by vacuum distillation before storage.

2.2. Techniques

Catalytic activity tests were carried out using a glass flow tubular reactor system loaded with *ca.* 4 g of sample. Catalyst particles in the 0.125–0.250 mm range were selected after pelleting, grinding and sieving in order to minimize the pressure drop and internal diffusion effects while the reactor geometry was optimized to avoid significant external diffusion effects. Analysis of the feed and outlet gas streams was performed using a Perkin–Elmer FTIR spectrometer model 1725X, coupled to a multiple reflection transmission cell (Infrared Analysis Inc. "long path gas minicell", 2.4 m path length, *ca.* 130 cm^3 internal volume); the O_2 concentration in the gas stream was determined with a paramagnetic analyzer (Servomex 540 A). Prior to catalytic testing, the catalysts were subjected to a standard calcination pretreatment using 3% O_2/N_2 flow at 773 K for 1 h, cooling to room temperature (RT) in the same flow, and finally briefly purging in N_2. The catalytic tests were performed under stoichiometric conditions in 1% CO and 0.5% O_2 or 1% CO, 0.45% O_2 and 0.1% NO, using N_2 as carrier gas at atmospheric pressure and a total flow of 1.5×10^3 cm^3 min^{-1} (roughly corresponding to 3×10^4 h^{-1} GHSV) and temperature ramps of 5 K min^{-1}; analysis of the bypass flow showed that around 45 ppm of NO_2 are present at RT in the latter gas mixture under these experimental conditions, due to partial homogeneous NO/NO_2 equilibration. In all cases, the runs were commenced after an initial equilibration period of *ca.* 5 min in the reactant flow at RT.

Diffuse reflectance infrared Fourier transform spectroscopy (DRIFTS) analysis under reaction conditions was done using a Perkin–Elmer 1750 FTIR spectrometer equipped with an MCT detector. The spectra were taken at 4 cm^{-1} resolution and accumulating 10 scans for every spectrum. The DRIFTS cell (Harrick) was fitted with CaF_2 windows and a heating cartridge which allowed samples to be heated up to 773 K. Samples of *ca.* 80 mg were calcined *in situ* (in a similar manner to the catalytic activity tests) and then cooled to RT before introducing the reaction mixture (passing through the catalyst bed) consisting of 1% CO and 0.5% O_2 or 1% CO, 0.45% O_2 and 0.1% NO in N_2, and using a total flow of *ca.* 80 cm^3 min^{-1}. The temperature was increased in a stepped manner using ramps of 5 K min^{-1}, stopping at the recording temperature and maintaining it during the course of the recording. A computer controlled gas blender was used to monitor the composition of the inlet gases. On-line analyses of the reaction products was done by mass spectrometry (Balzers Prisma QMS) and a chemiluminescence detector (Thermo Environmental Instruments 42C).

Electron paramagnetic resonance (EPR) spectra were recorded at 77 K with a Bruker ER 200 D spectrometer operating in the X-band and calibrated with a DPPH standard ($g = 2.0036$). Portions of about 30 mg of sample were placed inside a quartz probe cell with greaseless stopcocks using a conventional high vacuum line (capable of maintaining a dynamic vacuum of *ca.* 6×10^{-3} N m^{-2}) for the different treatments. In all cases, the sample was pretreated in 300 Torr (1 Torr = 133 N m^{-2}) of pure oxygen at 773 K for 2 h. CO reduction treatments at a specific reduction temperature (T_r) were made under static conditions using 100 Torr of CO, heating for 1 h at the corresponding T_r and subsequently outgassing at the same temperature for 0.5 h. Quantitative determination of the amount of species present in the spectra was performed by double integration of the corresponding EPR spectra and comparison with a copper sulfate standard.

3. Results and discussion

Multitechnique characterization of the CuC catalyst has been reported in previous works [6,30–32]. In brief, CuC displays specific surface area $S_{BET} = 92$ m^2 g^{-1}. All copper in the initial calcined sample appears fully oxidised (Cu^{2+} state) on the basis of XPS and XANES [30–32]. EPR analysis suggests that around 40% of the Cu^{2+} forms small well dispersed copper oxide particles while the rest forms relatively large copper oxide particles which escape EPR detection as a

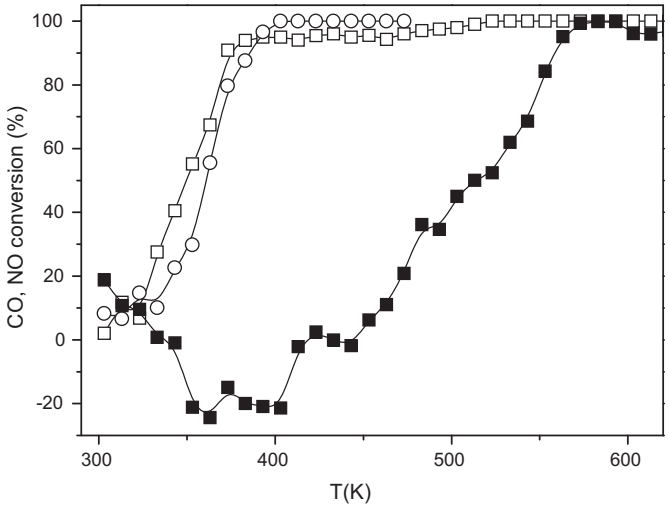

Fig. 1. Conversion profiles obtained during the CO–O_2 and CO–O_2–NO reaction over CuC. Circles: CO conversion; CO–O_2 reaction. Squares: CO–O_2–NO reaction; open: CO conversion; full: NO conversion.

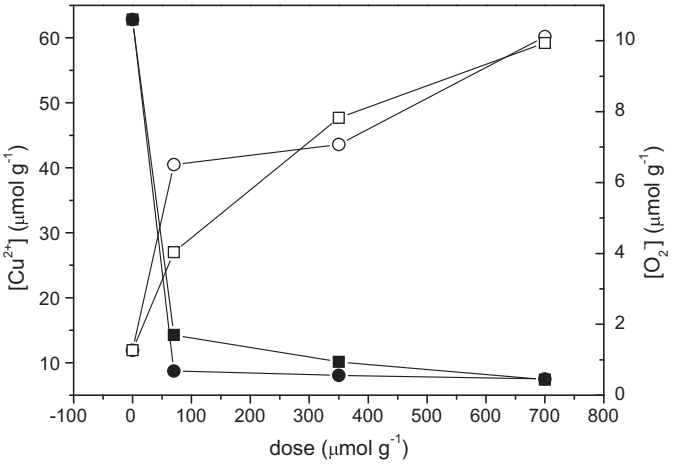

Fig. 2. Intensities of EPR signals due to Cu^{2+} species (open symbols) and Ce^{4+}–O_2 species (full symbols) as a function of the amount of O_2 (circles) or NO (squares) adsorbed at RT on CuC reduced under CO at T_r = 373 K.

consequence of antiferromagnetic coupling between Cu^{2+} cations. A residual amount appears as isolated Cu^{2+} [6,30]. Note the latter is based on very sensitive EPR technique exploration since no hint of copper oxide crystals could be detected by XRD or HREM, indicating an overall high dispersion degree of the CuO particles, in agreement with XPS analysis [6,30,32]. In turn, XRD, HREM and Raman reveal the presence of fluorite CeO_2 nanocrystals (*ca.* 8 nm average size) with more or less rounded shape, which act as support of the CuO particles [30,32].

The results of CO oxidation and NO reduction catalytic activity tests obtained under the CO–O_2 and CO–O_2–NO reactant mixtures are shown in Fig. 1. CO oxidation with O_2 apparently takes place at relatively low temperature since NO reduction does not occur in this catalyst until *ca.* 443 K with no N_2O formation being detected during the course of the reaction (i.e., NO reduction directly to N_2 must be produced). It can be noted that changes detected in the NO evolution at lower temperature must be attributed to a low temperature NO chemisorption (starting from room temperature and extending up to *ca.* 333 K) followed by NO desorption (as well as a residual amount of N_2O) up to *ca.* 413 K. It may be also noted the irregular shape of the NO conversion profile, with a turning point around 520 K, during the reduction of NO by CO (above *ca.* 443 K). This suggests a change in the reaction mechanism and/or the type of active sites during the course of the reaction, as will be analysed below.In any case, O_2 is considerably most powerful oxidant for CO than NO, according to results in Fig. 1. This can be rationalized on the basis of EPR results and assuming redox processes as being mainly responsible for the general catalytic features observed. Previous reports demonstrated in some detail the nature of the Cu^{2+} species observed in the EPR spectrum of CuC in its initial calcined state as well as the evolution of the species as a function of treatments under CO at different reduction temperatures [6,30]. As mentioned above, approximately 40% of the entire copper content was detected for the initial calcined sample, the spectrum being mainly formed by a featureless broad signal showing extremes at $g = 2.21$ and $g = 2.04$, attributed to Cu^{2+} cations in small copper oxide clusters. Additionally, a minor signal at $g_{||} = 2.233$ and $g_{\perp} = 2.036$ showing four-lines hyperfine splittings in each of its components with $A_{||} = 16.0 \times 10^{-3}\ cm^{-1}$ and $A_{\perp} = 1.8 \times 10^{-3}\ cm^{-1}$, attributed to isolated Cu^{2+} cations in a (generally speaking) tetragonally distorted octahedral symmetry is detected. The presence of weak features at $g = 2.26$ and 1.86 (corresponding to the splitting of the $g_{\perp}$ component at $g = 2.04$) reveal the presence of residual amounts of Cu^{2+} ionic pairs [33,34]. The portion of the copper which remains undetectable by EPR for the initial sample can be proposed to be related to antiferromagnetically coupled Cu^{2+} species (on the basis of XPS results showing that most of the copper appears as Cu^{2+} in the calcined sample [30]). Such antiferromagnetic arrangement of the Cu^{2+} cations can result from the presence of such cations into well ordered (in relatively large particles) CuO particles or from ceria-induced interactions [30]. A significant decrease in the Cu^{2+} intensity, affecting both signals present in the spectrum, was produced upon reduction of the sample under CO at RT and 373 K. Thus, *ca.* 24 and 8% of the entire copper loading was detected as Cu^{2+} after those experiments, respectively [6]. Exposure of the reduced sample to oxygen at 77 K led to the appearance of superoxide species chemisorbed on cerium cations (formally O_2^-–Ce^{4+} species) giving rise to signals at $g_z = 2.034$–2.029, $g_x = 2.016$ and $g_y = 2.011$ [16]. Formation of those species provided the principle evidence to indicate that support reduction had occurred, considering that paramagnetic Ce^{3+} species are not easily detectable by EPR due to their short spin-lattice relaxation time [27].

On the basis of those results, specific experimental protocols focused on determining by EPR the redox properties of CuC upon interaction with O_2 or NO. For that purpose, the initial calcined CuC sample was reduced under CO at 373 K (followed by outgassing at the same temperature). Then, increasing doses of either O_2 or NO were chemisorbed over that sample at RT (dose chemisorbed at 77 K followed by heating in the closed EPR cell at RT during 30 min), followed by thorough outgassing at the same temperature. The evolution of the Cu^{2+} signals (identified mainly as Cu^{2+} species within small copper oxide clusters) was then monitored during the reoxidation treatments. Following each of these treatments, the samples were exposed to O_2 (a dose of 70 μmol/g of catalyst) at 77 K (followed by outgassing at 77 K) and the evolution of O_2^-–Ce^{4+} signals formed upon such interaction was monitored. The results obtained are shown in Fig. 2. These results indicate that O_2 is a more powerful oxidant than NO for both copper and support sites reduced under CO.

Returning to conversion profiles of Fig. 1, it must be noted that the presence of NO in the reactant mixture apparently shifts CO conversion (related to CO oxidation with O_2, as discussed above) to lower temperature. To the best of our knowledge, this is first time such interesting effect of NO acting as gas promoter of CO oxidation has been revealed. This must not be attributed to differences in p_{CO}/p_{O_2} concentration ratios employed in the reactant stream (higher in the presence of NO) since it is well known that reaction order with respect to O_2 during CO oxidation is practi-

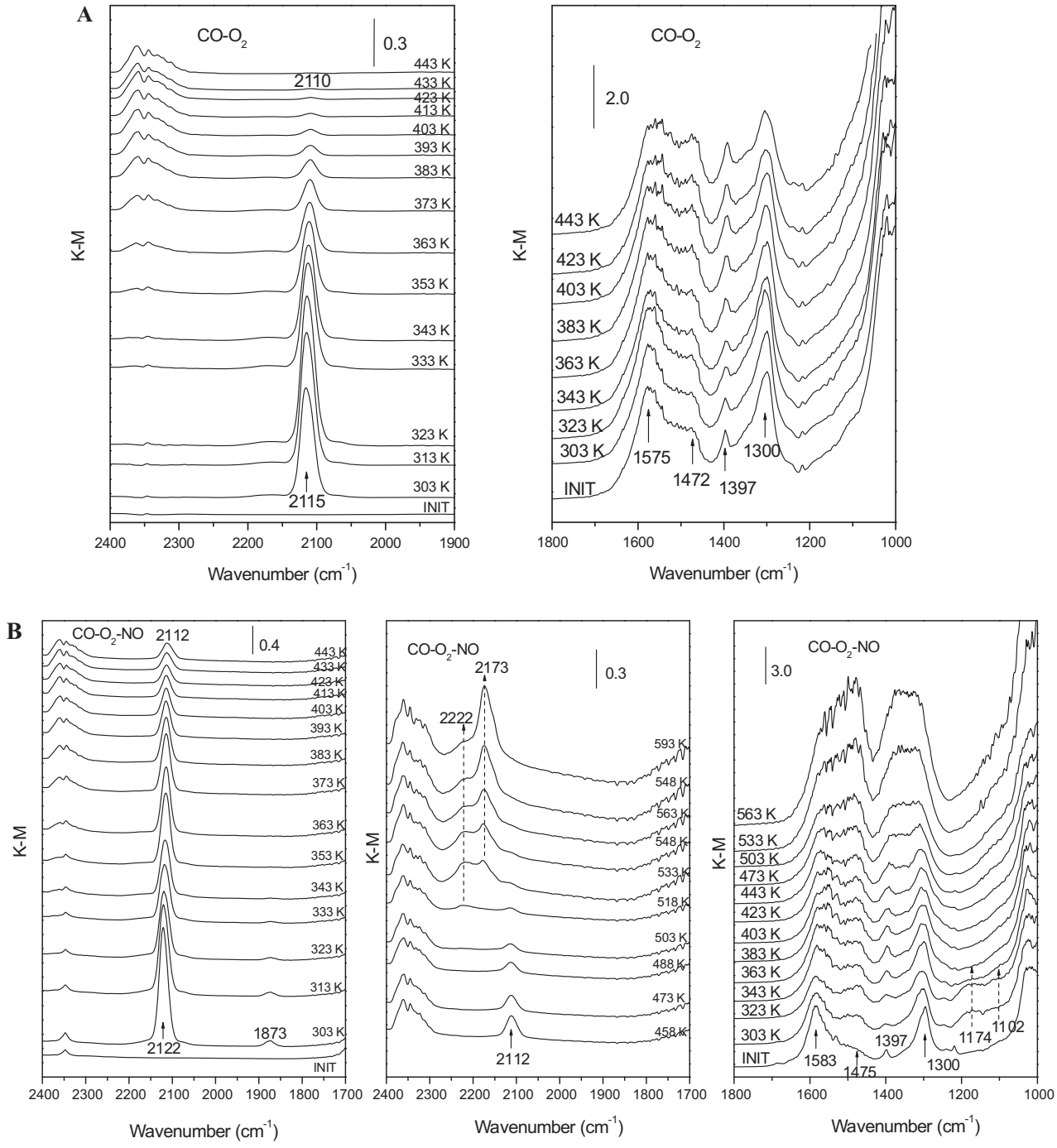

Fig. 3. *In situ*-DRIFTS spectra of CuC at the indicated temperatures (INIT corresponds to the spectrum recorded under N_2 after pretreatment under diluted O_2 at 773 K and prior to introduction of the reactant mixture) (A) $CO–O_2$ (B) $CO–O_2–NO$.

cally zero over this type of catalysts [18,19,35], which is reflected by the absence of differences in CO isoconversion temperature as a function of changes in p_{O_2} [35]. Such particular NO promoting effect appears exclusive of catalysts combining copper and cerium oxides and was apparently much less pronounced when the support was changed to Ce–Zr mixed oxide in an analogous catalyst [17]. In any case, such behaviour is just opposite to that observed over supported palladium catalysts in which the presence of NO (under the same experimental conditions) appreciably inhibits CO oxidation activity mainly as a consequence of hindered CO adsorption over palladium in the presence of coadsorbed NO species which delays attainment of active metallic palladium particles under the reactant mixture [36]; only in some particular case in which ceria–alumina was used as support of palladium, a low temperature enhancement of CO oxidation in the presence of NO has been detected although it has been related to contributions from CO–NO reaction rather than from $CO–O_2$ one [37,38].

In order to explore this effect as well as to achieve details of CO oxidation and NO reduction processes, CuC was examined by *operando*-DRIFTS. Spectra recorded at increasing temperatures under $CO–O_2$ or $CO–O_2–NO$ reaction conditions are shown in Fig. 3. Bands related to carbonyl species, chemisorbed CO_x- or NO_x-type species and hydroxyl species are observed in these spectra. Only the spectral regions corresponding to the two former type of species are displayed since evolution of hydroxyl species in the course of the runs does not appear of relevance in explaining the catalytic

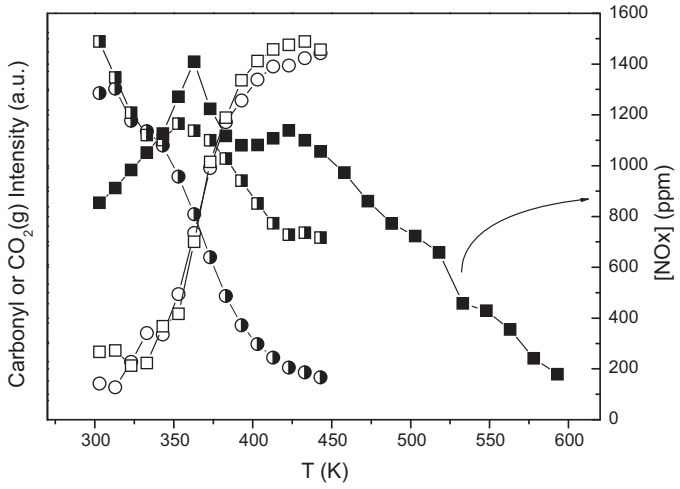

Fig. 4. Intensities observed by DRIFTS for the Cu^+ carbonyl at 2122–2110 cm^{-1} (half-filled symbols) and the CO_2(g) bands (open symbols) during the course of the $CO–O_2$ (circles) and $CO–O_2–NO$ (squares) reactions. Full squares represent the evolution of NO_x detected by chemiluminescence in the course of the $CO–O_2–NO$ reaction.

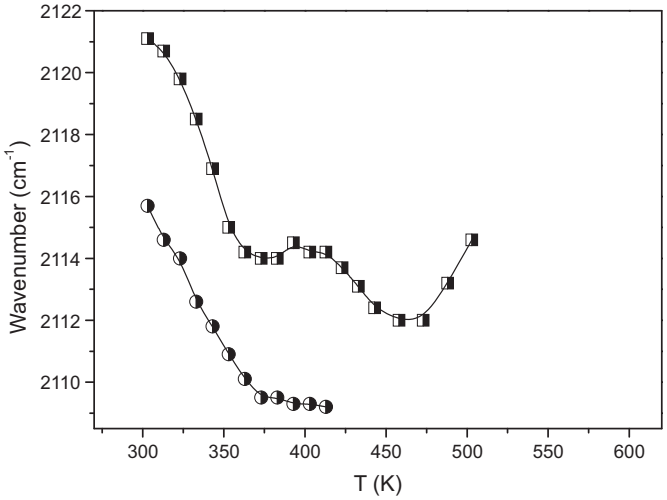

Fig. 5. Evolution of the frequency of the Cu^+-carbonyl species (see main text) as a function of reaction temperature under $CO–O_2$ (circles) and $CO–O_2–NO$ (squares).

results. First, it may be noted that a reasonable correlation is apparent between the evolution of gas phase CO_2 (appearing as relatively broad bands at 2400–2300 cm^{-1}) and the catalytic activity results (compare Figs. 3 and 1). Unfortunately, the low molar extinction coefficient and low concentration of NO(g) employed prevent its detection in the DRIFTS spectra under the conditions employed. Nevertheless, on-line NO_x monitoring by chemiluminescence confirmed the similarities between runs performed in the two types of experimental systems (Figs. 1 and 4), with in particular the presence of an irregularity at about 520 K in the NO_x conversion shape, similar to that observed during catalytic activity tests with the tubular reactor.

Concerning the carbonyl stretching region of the spectra, one band is observed in the 2122–2109 cm^{-1} range upon interaction with the reactant mixture. This band is characteristic of carbonyl species adsorbed on copper sites in contact with ceria [6,26]. It may be noted that although its frequency would appear somewhat low for a cationic copper adsorption site [39], previous experiments have shown its relatively high thermal stability [6,40], supporting its attribution to Cu^+ carbonyls. A gradual red shift of this band is observed with increasing the temperature under both reactant streams (from 2115 to 2109 cm^{-1} and 2122 to 2112 cm^{-1} under $CO–O_2$ and $CO–O_2–NO$, respectively, as displayed in Fig. 5. It must be noted that such frequency evolution is not explained on the basis of dipolar coupling effects between close packed carbonyl species, as shown in previous detailed analyses [17,40]). On the other hand, bands due to carbonate species (bidentate species giving most intense bands at *ca.* 1583–1575 and 1300 cm^{-1} and monodentate species giving the most intense bands at *ca.* 1475–1472 and 1397 cm^{-1} [40]; note the latter has been also attributed to polydentate carbonates, as discussed elsewhere [41]) are observed in the spectrum of the initial calcined sample. It must be noted that such species are difficult to eliminate by the pretreatment due to the strongly basic character of the ceria support. Generally speaking, an increase of bands due to monodentate carbonates is observed with increasing reaction temperature for both reactions. In addition, comparison between experiments in the presence and absence of NO (Fig. 2A and B) provided a means to distinguish the formation of bands resulting from NO_x adsorption or reaction. A band at 1873 cm^{-1} appeared instantly upon contact with the $CO–O_2–NO$ reactant mixture at 303 K and strongly decreased with increasing reaction temperature and was practically undetectable for $T > 353$ K. This band can be attributed to nitrosyl species adsorbed at exposed Cu^{2+} cations [42]. Additionally, bands at 1174 and 1102 cm^{-1} also appeared upon contact with the reactant mixture at 303 K, reaching maximum intensity at 313–323 K and decreasing strongly for $T \geq 363$ K. Perusal of Fig. 2B suggests the latter band reappears at 443 K. According to previous work (where details on the assignment can be found), these bands are attributed to, respectively, chelating nitrite and trans-hyponitrite species coordinated to cerium cations [27,43]. On the other hand, a band at *ca.* 2222 cm^{-1}, which is attributed to isocyanate (–NCO) species [29,44,45], is observed from *ca.* 518 K under $CO–O_2–NO$. Immediately after formation of such isocyanate species, a band at 2173 cm^{-1}, which can be related to ionic NCO^- chemisorbed on metallic copper [46–48], is observed and increases in intensity as a function of reaction temperature.

Evolution of the NO conversion profiles in Fig. 1 (employing the tubular catalytic reactor) and 4 (using the DRIFTS cell) can be rationalized on the basis of DRIFTS results (Fig. 3B). Initial NO adsorption and subsequent desorption produced up to *ca.* 380 K correlates with evolution observed in chelating nitrite or hyponitrite species chemisorbed on ceria or nitrosyls formed over CuO. Then, NO reduction by CO observed from about 425 K involves an initial stage up to *ca.* 520 K during which, active sites can be related to reduced cerium entities giving rise to hyponitrite species upon NO chemisorption which can decompose to nitrogen with simultaneous ceria reoxidation [27,43]. Onset of the second part of the profile of NO reduction by CO (from *ca.* 520 K) coincides with formation of isocyanate species, most likely formed over metallic copper. This suggests that the latter can provide active sites for NO dissociation giving rise to isocyanate species upon further interaction with CO [49]. It may be noted that the presence of well differentiated steps, involving different active sites and mechanisms, during NO reduction by CO appears characteristic for this type of catalysts, as shown in a previous report [29]. Furthermore, changes in the rate of NO reduction by CO (typically under CO + NO reactant mixture) have been also observed for Pd or Pt catalysts in the presence of CeO_2 (or isostructural Ce–Zr mixed oxide) [50,51], being apparently absent when the latter is not present [51]. This has been proposed to be related to the existence of a low temperature NO reduction path in which interfacial activation of NO by cerium cations, as a consequence of its redox activity, can take place [51].

Let us now focus our attention on the NO promoting effect on CO oxidation. For this, the evolution of the intensity of the Cu^+-carbonyl band as a function of the reaction temperature in the

presence and absence of NO in the reactant mixture is displayed in Fig. 4. The evolution of CO_2(g) in the DRIFTS spectra, reflecting CO oxidation activity, during both tests is also shown in Fig. 4. Even though it is difficult to extract differences between both CO_2(g) evolution profiles, it appears clear that CO oxidation progresses to a slightly greater extent in the presence of NO. On the other hand, noteworthy, differences are observed in the evolution of the band intensity of Cu^+ carbonyls between both experiments. In particular, while the band intensity shows a maximum at 313 K under CO–O_2, two maxima (at 303 and 353 K) are present under CO–O_2–NO. In turn, it is worth noting that the intensity increase giving rise to the second maximum under CO–O_2–NO closely correlates with the onset of CO oxidation and with NO desorption from nitrite or nitrosyl species. According to previous studies [6,15,30,32], the intensity of these Cu^+ carbonyl species reflects the reduction of interfacial copper oxide centres under the reactant stream, assuming that the catalyst starts from a fully oxidised state, as mentioned above. CO oxidation rate has been shown to be proportional to the level of copper oxide reduction achieved at such interfacial zones, the intensity of Cu^+-carbonyls formed prior to reaction onset acting thus as a relevant fingerprint of CO oxidation activity [15,16]. In this case, fairly similar intensities of Cu^+ carbonyls are observed upon first contact of the two reactant mixtures with the catalyst, thus reflecting similar reduction levels are achieved at copper oxide interfacial sites. CO apparently chemisorbs stronger than NO on Cu^+ sites generated upon such initial reductive interaction with the reactant mixture. Note in this sense that Cu^+ nitrosyl species, which are expected to give rise to bands around 1780 cm^{-1}, i.e. appreciably red shifted with respect to those formed on Cu^{2+} sites [17], are not formed under reaction conditions (Fig. 3B). In any case, the formation of Cu^{2+} nitrosyls (band at 1873 cm^{-1}) and their interaction with neighbouring Cu^+ carbonyls may well be responsible for the general blue shift detected in Cu^+ carbonyls in the presence of NO (Fig. 5). In any case, the important increase in the number of interfacial Cu^+ sites produced in the presence of NO between about 333 and 400 K indicates, following previously arguments, that an important increase in the number of interfacial active sites is produced, which explains the promoting effect of NO on CO oxidation. Since such an increase coincides with NO_x desorption from chemisorbed nitrites (on ceria) or nitrosyls (on CuO), it appears likely that both phenomena are intimately related. It must be noted that in any case differences in respective Cu^+-carbonyl intensities (in the presence or absence of NO) are not most likely affected by differences in the ν(CO) absorption coefficient in each case. In this sense, a recent detailed analysis of $Au/Ce_{0.6}Zr_{0.4}O_2$ indicates an important dependence of ν(CO) absorption coefficient in metallic gold carbonyls as a function of the redox state, either oxidised or reduced, of the support [52]. However, in our case, no significant difference is expected in this sense while frequency differences appear relatively small (Fig. 5), thus suggesting absorption coefficients of Cu^+-carbonyls detected in each case should be fairly similar. On the other hand, careful analysis of Figs. 1 and 4 suggests that CO oxidation onset is triggered at a slightly lower temperature in the absence of NO, this latter being apparently produced (when NO is present) only when desorption of NO_x from nitrite or nitrosyl species takes place. This suggests the presence of such NO_x derived chemisorbed species somewhat deactivates the interface during the initial stages. Their desorption most likely activates interfacial oxygens making them more reducible and increasing the amount of active Cu^+ sites formed upon interaction with CO in the reactant mixture. It is difficult to resolve which of such NO_x-derived chemisorbed species can be responsible for the effect on the basis of the results obtained. According to previous studies [27,43], chelating nitrite species are formed upon interaction of NO with coordinatively unsaturated Ce^{4+} centres while hyponitrite species are formed upon NO interaction with close reduced cerium centres (Ce^{3+}) on which associated oxygen vacancies become exposed. The latter species has been proposed to be the main intermediate involved in NO reduction over reduced ceria since hyponitrite species apparently decompose to N_2O or N_2 [27], leaving the ceria surface partially or fully oxidised. In turn, chelating nitrite species could in principle decompose back to NO or alternatively to NO_2 [53], the latter inducing ceria reduction. This latter reducing step along with existence of $Ce^{3+} \rightarrow Cu^{2+}$ interfacial electron transfer effects could explain the observed increase observed in the amount of Cu^+ carbonyls. Nevertheless, we cannot discard that neutral or oxidative desorption of observed nitrosyls, chelating nitrites or hyponitrite species could activate interfacial oxygens making them more readily reducible. Further experiments are certainly required to achieve more precise details that could explain to a deeper level the NO-promoting effect observed.

4. Conclusions

A catalyst of copper oxide supported on ceria has been examined with respect to its catalytic properties for CO oxidation with either O_2 alone or O_2 + NO. A promoting effect of NO on CO oxidation by O_2 has been revealed and rationalized on the basis of *operando*-DRIFTS results. It is shown that NO undergoes a process of adsorption at low temperature giving place to species chemisorbed on the CuO component (nitrosyls) or the CeO_2 one (chelating nitrite and hyponitrite species); their subsequent desorption below *ca.* 443 K apparently activates the interfacial zone active for CO oxidation by O_2 facilitating to attain a higher degree of reduction in it which may explain the mentioned promoting effect. In turn, details of NO reduction are achieved by *operando*-DRIFTS showing the existence of a discontinuity during the course of the reaction which is explained on the basis of a change of the type of active site/mechanism. The results are complemented by EPR analysis of redox properties which evidence the higher oxidizing power of O_2 with respect to NO for any of the two catalyst components (CuO and ceria).

Acknowledgements

Thanks are due to Mr. F. Sánchez Constenla for performing a part of the EPR experiments. Financial support by the MICINN (Project CTQ2009-14527) and Comunidad de Madrid (Project DIVERCEL S2009/ENE-1475) is acknowledged.

References

[1] A. Trovarelli, Catal. Rev. Sci. Eng. 38 (1996) 439.
[2] S. Park, J.M. Vohs, R.J. Gorte, Nature 404 (2000) 265.
[3] S. Bernal, J.J. Calvino, J.M. Gatica, C. López Cartes, J.M. Pintado, in: A. Trovarelli (Ed.), Catalysis by Ceria and Related Materials, Imperial College Press, London, 2001, p. 85.
[4] W. Liu, A.F. Sarofim, M. Flytzani-Stephanopoulos, Chem. Eng. Sci. 49 (1994) 4871.
[5] M.-F. Luo, Y.-J. Zhong, X.-X. Yuan, X.-M. Zheng, Appl. Catal. A 162 (1997) 121.
[6] A. Martínez-Arias, M. Fernández-García, O. Gálvez, J.M. Coronado, J.A. Anderson, J.C. Conesa, J. Soria, G. Munuera, J. Catal. 195 (2000) 207.
[7] P.W. Park, J.S. Ledford, Catal. Lett. 50 (1998) 41.
[8] P. Bera, A.T. Aruna, K.C. Patil, M.S. Hegde, J. Catal. 186 (1999) 36.
[9] J.B. Wang, W.-H. Shih, T.-J. Huang, Appl. Catal. A 203 (2000) 191.
[10] X.Q. Wang, J.A. Rodriguez, J.C. Hanson, D. Gamarra, A. Martinez-Arias, M. Fernandez-Garcia, J. Phys. Chem. B 110 (2006) 428.
[11] X.Q. Wang, J.A. Rodriguez, J.C. Hanson, D. Gamarra, A. Martinez-Arias, M. Fernandez-Garcia, Top. Catal. 49 (2008) 7.
[12] L. Barrio, M. Estrella, G. Zhou, W. Wen, J.C. Hanson, A.B. Hungría, A. Hornés, M. Fernández-García, A. Martínez-Arias, J.A. Rodriguez, J. Phys. Chem. C 114 (2010) 3580.
[13] P.G. Harrison, I.K. Ball, W. Azelee, W. Daniell, D. Goldfarb, Chem. Mater. 12 (2000) 3715.
[14] D.-H. Tsai, T.-J. Huang, Appl. Catal. A 223 (2002) 1.
[15] D. Gamarra, C. Belver, M. Fernández-García, A. Martínez-Arias, J. Am. Chem. Soc. 129 (2007) 12064.
[16] C.S. Polster, H. Nair, C.D. Baertsch, J. Catal. 266 (2009) 308.

[17] A. Martínez-Arias, M. Fernández-García, A.B. Hungría, A. Iglesias-Juez, O. Gálvez, J.A. Anderson, J.C. Conesa, J. Soria, G. Munuera, J. Catal. 214 (2003) 261.
[18] G. Sedmak, S. Hocevar, J. Levec, J. Catal. 213 (2003) 135.
[19] A. Martínez-Arias, D. Gamarra, M. Fernández-García, A. Hornés, C. Belver, Top. Catal. 52 (2009) 1425.
[20] J.B. Wang, D.-H. Tsai, T.-J. Huang, J. Catal. 208 (2002) 370.
[21] A. Martínez-Arias, D. Gamarra, M. Fernández-García, X.Q. Wang, J.C. Hanson, J.A. Rodriguez, J. Catal. 240 (2006) 1.
[22] A. Hornés, A.B. Hungría, P. Bera, A. López Cámara, M. Fernández-García, A. Martínez-Arias, L. Barrio, M. Estrella, G. Zhou, J.J. Fonseca, J.C. Hanson, J.A. Rodriguez, J. Am. Chem. Soc. 132 (2010) 34.
[23] A. Martínez-Arias, D. Gamarra, M. Fernández-García, A. Hornés, P. Bera, Zs. Koppány, Z. Schay, Catal. Today 143 (2009) 211.
[24] A.-P. Jia, S.-Y. Jiang, J.-Q. Lu, M.-F. Luo, J. Phys. Chem. C 114 (2010) 21605.
[25] M.-F. Luo, X.-M. Zheng, Acta Chem. Scand. 52 (1998) 1183.
[26] A. Martínez-Arias, M. Fernández-García, J. Soria, J.C. Conesa, J. Catal. 182 (1999) 367.
[27] A. Martínez-Arias, J. Soria, J.C. Conesa, X.L. Seoane, A. Arcoya, R. Cataluña, J. Chem. Soc. Faraday Trans. 91 (1995) 1679.
[28] J. Chen, Y. Zhan, J. Zhu, C. Chen, X. Lin, Q. Zheng, Appl. Catal. A 377 (2010) 121.
[29] R. Zhang, W.Y. Teoh, R. Amal, B. Chen, S.J. Kaliaguine, Catalysis 272 (2010) 210.
[30] A. Martínez-Arias, A.B. Hungría, M. Fernández-García, J.C. Conesa, G. Munuera, J. Phys. Chem. B 108 (2004) 17983.
[31] A. Martínez-Arias, A.B. Hungría, M. Fernández-García, J.C. Conesa, G. Munuera, J. Power Sources 151 (2005) 32.
[32] D. Gamarra, G. Munuera, A.B. Hungría, M. Fernández-García, J.C. Conesa, P.A. Midgley, X.Q. Wang, J.C. Hanson, J.A. Rodríguez, A. Martínez-Arias, J. Phys. Chem. C 111 (2007) 11026.
[33] A. Abou Kaïs, A. Bennani, C.F. Aïssi, G. Wrobel, M. Guelton, J. Védrine, J. Chem. Soc. Faraday Trans. 88 (1992) 615.
[34] J. Soria, J.C. Conesa, A. Martínez-Arias, J.M. Coronado, Solid State Ionics 63–65 (1993) 755.
[35] H.C. Lee, D.H. Kim, Catal. Today 132 (2008) 109.
[36] A.B. Hungría, M. Fernández-García, J.A. Anderson, A. Martínez-Arias, J. Catal. 235 (2005) 262.
[37] A. Iglesias-Juez, A. Martínez-Arias, A.B. Hungría, J.A. Anderson, J.C. Conesa, J. Soria, M. Fernández-García, Appl. Catal. A 259 (2004) 207.
[38] A. Iglesias-Juez, PhD Thesis, Universidad Autónoma de Madrid, 2004.
[39] P. Hollins, Surf. Sci. Rep. 16 (1992) 51.
[40] P. Bera, A. López Cámara, A. Hornés, A. Martínez-Arias, J. Phys. Chem. C 113 (2009) 10689.
[41] C. Binet, M. Daturi, J.-C. Lavalley, Catal. Today 50 (1999) 207.
[42] A.A. Davydov, in: C.H. Rochester (Ed.), Infrared Spectroscopy of Adsorbed Species on the Surface of Transition Metal Oxides, John Wiley & Sons, 1990, p. 75.
[43] A. Martínez-Arias, J.C. Conesa, J. Soria, Res. Chem. Interm. 33 (2007) 775.
[44] J.W. Labdon, A.T. Bell, J. Catal. 31 (1973) 96.
[45] J.A. Anderson, C.H. Rochester, J. Chem. Soc., Faraday Trans. 1 85 (1989) 1117.
[46] J. Raskó, F. Solymosi, J. Catal. 71 (1981) 219.
[47] F. Solymosi, T. Bansagi, J. Catal. 156 (1995) 75.
[48] A. Iglesias-Juez, A. Martínez-Arias, M. Fernández-García, J. Catal. 221 (2004) 148.
[49] B.-Z. Sun, W.-K. Chen, Y.-J. Xu, J. Chem. Phys. 131 (2009) 174503.
[50] J.A. Botas, M.A. Gutiérrez-Ortiz, M.P. González-Marcos, J.A. González-Marcos, J.R. González-Velasco, Appl. Catal. B 32 (2001) 243.
[51] R. Di Monte, J. Kaspar, P. Fornasiero, M. Graziani, C. Pazé, G. Gubitosa, Inorg. Chim. Acta 334 (2002) 318.
[52] J.M. Cíes, E. del Río, M. López-Haro, J.J. Delgado, G. Blanco, S. Collins, J.J. Calvino, S. Bernal, Angew. Chem. Int. Ed. 49 (2010) 9744.
[53] R. Cataluña, A. Arcoya, X.L. Seoane, A. Martínez-Arias, J.M. Coronado, J.C. Conesa, J. Soria, L.A. Petrov, Stud. Surf. Sci. Catal. 96 (1995) 215.